

A lithium ion battery exploiting a composite Fe₂O₃ anode and a high voltage

Li_{1.35}Ni_{0.48}Fe_{0.1}Mn_{1.72}O₄ cathode

Roberta Verrelli¹, Rosaria Brescia², Alice Scarpellini², Liberato Manna², Bruno Scrosati² and Jusef Hassoun^{1,*}

¹ Sapienza, University of Rome, Chemistry Department, 00185, Rome, Italy

² Department of Nanochemistry, Istituto Italiano di Tecnologia (IIT), Via Morego 30, 16163 Genova, Italy

SUPPLEMENTARY INFORMATION

A comparison of the structural and electrochemical properties of the Li_{1.35}Ni_{0.48}Fe_{0.1}Mn_{1.72}O₄ and the bare LiNi_{0.5}Mn_{1.5}O₄ [1], used as the reference cathode, is here reported in order to shed light on the effects of Fe-doping on the performances of the spinel electrode.

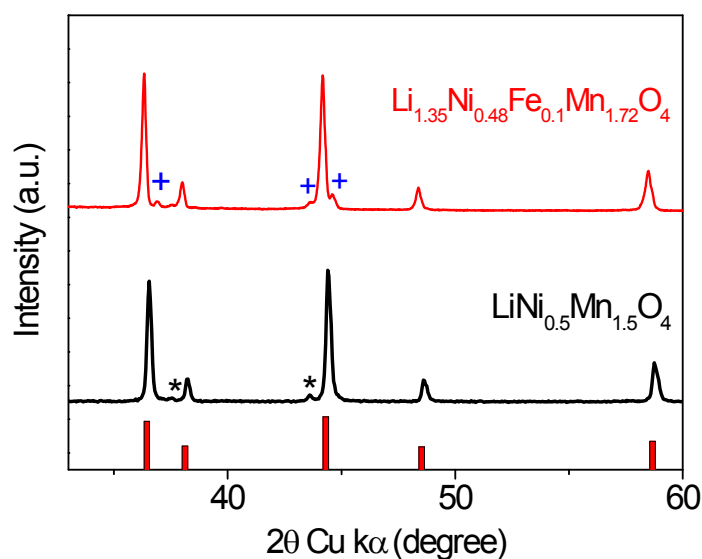


Figure S1

Figure S1 displays the XRD patterns of the undoped LiNi_{0.5}Mn_{1.5}O₄ and the Fe-substituted Li_{1.35}Ni_{0.48}Fe_{0.1}Mn_{1.72}O₄ powders.

The XRD patterns show the characteristic signals of the spinel, Fd-3m phase (JCPDS n. 802162).

The peaks at about 37.6° and 43.5°, marked with asterisks in the LiNi_{0.5}Mn_{1.5}O₄ diffractogram, may be attributed to the presence of a Li_xNi_{1-x}O impurity phase, as reported in literature papers [2-4].

As expected, the $\text{Li}_x\text{Ni}_{1-x}\text{O}$ impurity phase can be barely detected in the $\text{Li}_{1.35}\text{Ni}_{0.48}\text{Fe}_{0.1}\text{Mn}_{1.72}\text{O}_4$ pattern. According to literature data [4,5], partial substitution of Mn and Ni with other cations can reduce the amount of impurities formed during the synthesis of the spinel electrode.

Moreover an additional phase in the $\text{Li}_{1.35}\text{Ni}_{0.48}\text{Fe}_{0.1}\text{Mn}_{1.72}\text{O}_4$ pattern, with signals at about 36.9° , 43.6° and 44.6° (blue crosses in Fig.S1) can be detected. These signals may be most reasonably assigned to a mixed $\text{Li}_x\text{Ni}_y\text{Fe}_w\text{O}_z$ phase.

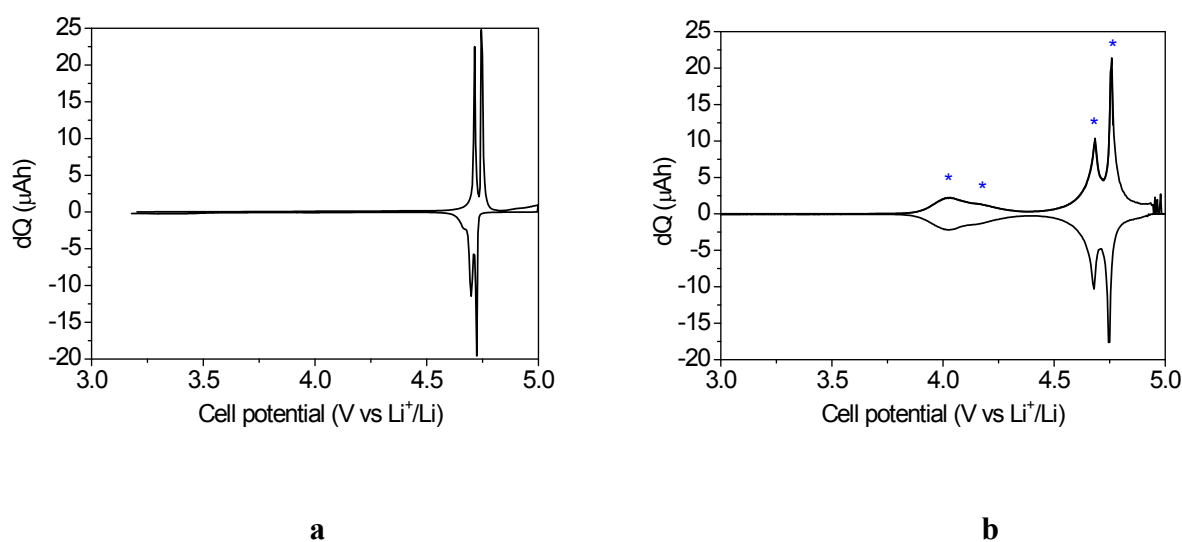


Figure S2

The results of Potentiodynamic Cycling with Galvanostatic Acceleration (PCGA) tests on a Li / LiPF_6 1M, EC:DMC 1:1/ $\text{LiNi}_{0.5}\text{Mn}_{1.5}\text{O}_4$ and a Li/ LiPF_6 1M, EC:DMC 1:1/ $\text{Li}_{1.35}\text{Ni}_{0.48}\text{Fe}_{0.1}\text{Mn}_{1.72}\text{O}_4$ cell are shown in Figure S2 a and S2 b, respectively.

Both the $\text{LiNi}_{0.5}\text{Mn}_{1.5}\text{O}_4$ and the $\text{Li}_{1.35}\text{Ni}_{0.48}\text{Fe}_{0.1}\text{Mn}_{1.72}\text{O}_4$ profiles show the signals associated to the $\text{Ni}^{2+}/\text{Ni}^{3+}$ and the $\text{Ni}^{3+}/\text{Ni}^{4+}$ redox couples, respectively at 4.71 and 4.75 V vs Li^+/Li and at 4.68 and 4.76 V vs Li^+/Li (The corresponding reduction processes can be noticed at 4.69 and 4.73 V vs Li^+/Li and at 4.68 and 4.75 V vs Li^+/Li , respectively).

The $\text{Li}_{1.35}\text{Ni}_{0.48}\text{Fe}_{0.1}\text{Mn}_{1.72}\text{O}_4$ electrode shows two additional redox processes at about 4 and 4.17 V vs Li^+/Li . As already discussed in the manuscript (see Fig. 4a discussion), iron-doping may alter

the Mn^{3+} ions concentration, thus inducing the appearance of a redox process at about 4V vs Li^+/Li , attributed to the $\text{Mn}^{3+}/\text{Mn}^{4+}$ redox couple.

Moreover oxygen deficiencies in the cathode structure, possibly formed during the synthetic annealing step, can account for the increase of Mn^{3+} concentration for ensuring charge neutrality.

The signal at about 4.17 V and 4.16 V vs Li^+/Li in the anodic and cathodic scan, respectively, can be attributed to the $\text{Fe}^{2+}/\text{Fe}^{3+}$ redox couple and, partially, to a possible shift of the 4 V oxidation peak of Mn^{3+} to higher potentials induced by Fe-doping [6].

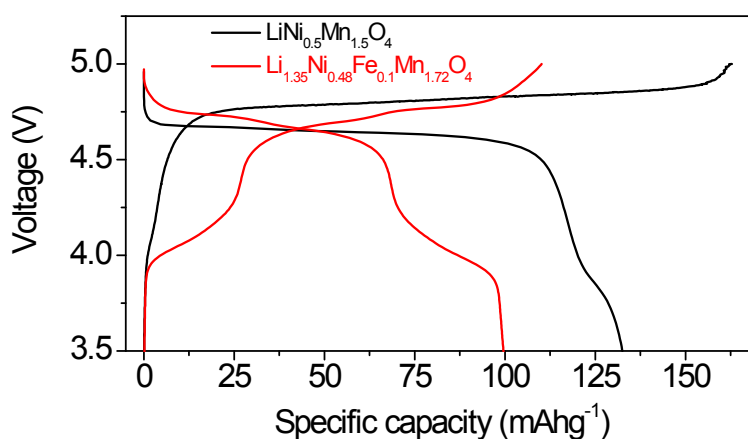


Figure S3

A comparison of the $\text{LiNi}_{0.5}\text{Mn}_{1.5}\text{O}_4$ and $\text{Li}_{1.35}\text{Ni}_{0.48}\text{Fe}_{0.1}\text{Mn}_{1.72}\text{O}_4$ galvanostatic cycling responses in terms of voltage versus specific capacity profiles is shown in Figure S3. As already pointed out in the discussion of the PCGA profiles (Figure S2), the doped $\text{Li}_{1.35}\text{Ni}_{0.48}\text{Fe}_{0.1}\text{Mn}_{1.72}\text{O}_4$ electrode shows a multi-step voltage profile, characterized by two main working regions, i.e. one between 4 and 4.25 V and the other between 4.6 and 4.8 V. The spinel cation substitution with iron ions induces a remarkable increase of the capacity delivered at the low voltage working region, due to the $\text{Mn}^{3+}/\text{Mn}^{4+}$ and $\text{Fe}^{2+}/\text{Fe}^{3+}$ redox couples. The capacity delivered by the $\text{Li}_{1.35}\text{Ni}_{0.48}\text{Fe}_{0.1}\text{Mn}_{1.72}\text{O}_4$ and the $\text{LiNi}_{0.5}\text{Mn}_{1.5}\text{O}_4$ cathodes in the 4 - 4.25 V region is about 25 mAh g^{-1} and 5 mAh g^{-1} , respectively.

Moreover the $\text{Li}_{1.35}\text{Ni}_{0.48}\text{Fe}_{0.1}\text{Mn}_{1.72}\text{O}_4$ galvanostatic cycling profile in the high voltage working region evolves with a multi-step, sloppy trend while the undoped $\text{LiNi}_{0.5}\text{Mn}_{1.5}\text{O}_4$ shows a plateau-like curve, that is characteristic of solid solution Lithium intercalation processes.

Although decreasing the energy density, the reduction of the electrode operating voltage to lower values improves the cell stability and safety level upon cycling by avoiding electrolyte decomposition.

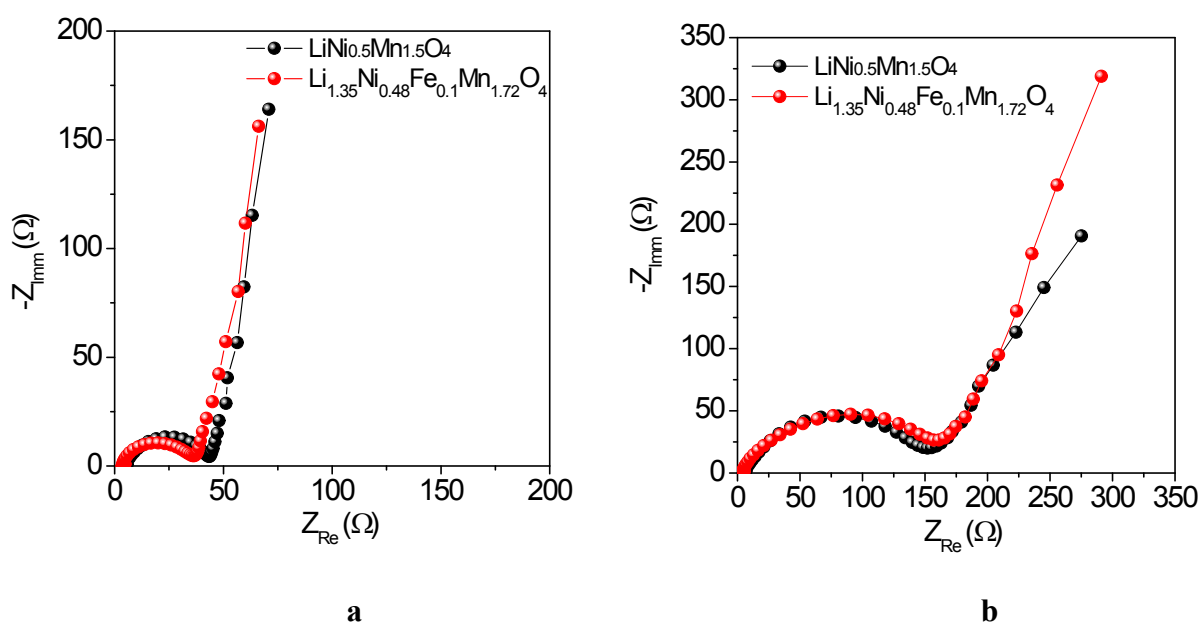


Figure S4

The electrode-electrolyte interface of the $\text{LiNi}_{0.5}\text{Mn}_{1.5}\text{O}_4$ and $\text{Li}_{1.35}\text{Ni}_{0.48}\text{Fe}_{0.1}\text{Mn}_{1.72}\text{O}_4$ cathodes is investigated by Electrochemical Impedance Spectroscopy (EIS). Figures S4 a and S4 b display the Nyquist plots of the Li/LiPF_6 1M, EC:DMC 1:1/ $\text{LiNi}_{0.5}\text{Mn}_{1.5}\text{O}_4$ and Li/LiPF_6 1M, EC:DMC 1:1/ $\text{Li}_{1.35}\text{Ni}_{0.48}\text{Fe}_{0.1}\text{Mn}_{1.72}\text{O}_4$ half-cells before and after a galvanostatic cycle, respectively. The equivalent circuit adopted for fitting the Nyquist plots is $R_{el}(R_{int}Q_{int})Q$, where R_{el} indicates the electrolyte resistance, R_{int} and Q_{int} correspond to the resistance and constant phase element (CPE) associated to the electrode/electrolyte interface and Q accounts for the diffusion of Li-ions in the low frequency range and the cell geometric capacity. The $(R_{int}Q_{int})$ element includes the

contribution of the resistance and capacitance associated both with the formation of a passivation film at the electrode surface and the charge transfer process.

Figures S4 a and b reveal only minor change of the cell impedance before and after cycling using both $\text{LiNi}_{0.5}\text{Mn}_{1.5}\text{O}_4$ and $\text{Li}_{1.35}\text{Ni}_{0.48}\text{Fe}_{0.1}\text{Mn}_{1.72}\text{O}_4$ electrodes. These results evidence that the presence of the iron doping in the spinel-structure doesn't affect remarkably the electrode/electrolyte interface properties.

The resistance values determined by fitting the EIS data are about $40\ \Omega$ and $32\ \Omega$ for the pristine $\text{LiNi}_{0.5}\text{Mn}_{1.5}\text{O}_4$ and $\text{Li}_{1.35}\text{Ni}_{0.48}\text{Fe}_{0.1}\text{Mn}_{1.72}\text{O}_4$ electrodes, respectively. After the charge-discharge cycle the cathodes show interface resistance of about $148\ \Omega$ and $157\ \Omega$, respectively. Further studies are required in order to investigate the effects of cation substitution on the properties of the solid electrode-electrolyte interface (SEI).

Experimental: Table S1

Table S1 lists the results of the ICP analysis on the $\text{Li}_{1.35}\text{Ni}_{0.48}\text{Fe}_{0.1}\text{Mn}_{1.72}\text{O}_4$ material .

Element	Wavelength	SD	%RSD	Int(c/s)	Calc. Conc.
Li	670.78	0.0125	1.2	45948.0	1.0283 ppm
Fe	238.204	0.0012	0.2	3857.8	0.6138 ppm
Mn	257.610	0.2507	2.4	401111.0	10.413 ppm
Ni	231.604	0.0198	0.6	3331.4	3.0636 ppm

References

[1] P. Reale, S. Panero, B. Scrosati, Sustainable High-Voltage Lithium Ion Polymer Batteries, *Journal of The Electrochemical Society* **2005**, 152, 10, A1949.

- [2] Y-P. Zeng, X-I. Wu, P. Mei, L-N. Cong, C. Yao, R-S-Wang, H-M. Xie, L-Q. Sun, Effect of cationic and anionic substitution on the electrochemical properties of $\text{LiNi}_{0.5}\text{Mn}_{1.5}\text{O}_4$ spinel cathode material, *Electrochimica Acta* **2014**, 138, 493.
- [3] T. F. Yi, B. Chen, Y-R. Zhu, X-Y. Li, R-S. Zhu, Enhanced rate performance of molybdenum-doped spinel $\text{LiNi}_{0.5}\text{Mn}_{1.5}\text{O}_4$ cathode materials for lithium ion battery, *Journal of Power Sources* **2014**, 247, 778.
- [4] Liu J., Manthiram A., Understanding the Improved Electrochemical Performances of Fe-substituted 5V Spinel Cathode $\text{LiMn}_{1.5}\text{Ni}_{0.5}\text{O}_4$, *Journal of Physical Chemistry C* **2009**, 113, 15073.
- [5] J. S. Chae, M. R. Jo, Y.-I. Kim, D-K. Han, S-M. Park, Y-M. Kang, K. C. Roh, Kinetic favorability of Ru-doped $\text{LiNi}_{0.5}\text{Mn}_{1.5}\text{O}_4$ for high-power lithium-ion batteries, *Journal of Industrial and Engineering Chemistry* **2014** (dx.doi.org/10.1016/j.jiec.2014.04.003).
- [6] Fey G. T.-K., Lu C.-Z., Kumar T. P., Preparation and Electrochemical Properties of High-Voltage Cathode Materials, $\text{LiM}_y\text{Ni}_{0.5-y}\text{Mn}_{1.5}\text{O}_4$ (M=Fe, Cu, AL, Mg; $y= 0.0-0.4$), *Journal of Power Sources* **2003**, 115, 332-345.